ΔVLBI Spacecraft Tracking System Demonstration Part II: Data Acquisition and Processing

C. S. Christensen and B. Moultrie
Navigation Systems Section

and

P. S. Callahan, F. F. Donivan, and S. C. Wu
Tracking Systems and Application Section

A set of experiments in the use of Differential Very Long Baseline Interferometry (AVLBI) for spacecraft navigation have been completed. Data using both Voyager spacecraft and a single quasar were acquired during the Jupiter encounter time period. The data were processed and analyzed to assess the navigation accuracy of AVLBI. This article focuses on the data reduction and techniques for assessing data quality and consistency.

I. Introduction

This is the second article in a series describing the DSN development of an improved spacecraft navigation system using Very Long Baseline Interferometry (VLBI) techniques. The first article (Ref. 1) described the goals and design and planning of a demonstration of narrow-band AVLBI using data taken near the two Voyager encounters of Jupiter. This article includes a review of the demonstration plan. It discusses the data acquisition for the demonstration and the data processing steps followed. There is an emphasis on the techniques used for assessing data quality and consistency. Consistency of the AVLBI passes used in the demonstration is at the 0.5-μradian level rather than the 0.05-μradian level expected. Reasons for the discrepancy are discussed.

II. The Voyager Narrowband ΔVLBI Demonstration

VLBI data is obtained by two widely separated antennas simultaneously receiving and recording a signal from a single radio source. These recorded signals are brought together and correlated to obtain precise differential (between the stations) range (wideband VLBI) or differential range rate (narrow-band VLBI). Delta VLBI (AVLBI) involves differencing VLBI data taken from a spacecraft with VLBI data taken from an angularly nearby extragalactic radio source (EGRS). Differencing between sources improves accuracy by near cancellation of common errors sources such as those introduced by station electronics, clocks, transmission media, and station locations.

To obtain an angular measurement from narrow-band AVLBI, a "pass" of data nominally four to five hours in length is required. During a pass, data is collected alternately from each source, the EGRS and the spacecraft. Each burst of data from a single source is called a "scan." In this demonstration, each scan was seven minutes long. Passes for this demonstration utilized baselines between the Deep Space Stations (DSS) at Goldstone, California, and either Madrid, Spain, or Canberra, Australia. A more detailed background on AVLBI and its expected use in spacecraft navigation is contained in Refs. 1, 2, and 3.

The demonstration involved both Voyager spacecraft and a single EGRS, OJ 287. The EGRS was near the retrograde loop of each spacecraft, hence angularly close to both spacecraft for a period of almost a year (see Fig. 1). Though the spacecraft-EGRS angular separation was far from ideal, reaching 12 deg near the Voyager 1 encounter, it was felt that the advantage of using a single radio source throughout outweighed the disadvantage of the large separation. A wide separation between sources implies that errors due to media (troposphere and charged particles) may not cancel well in the differenced data. More will be said on media calibration and cancellation in Section IV.

The demonstration design is as follows: Narrow-band AVLBI passes were taken using Voyager 1 and OJ 287 before and after the encounter of the spacecraft with Jupiter. These data were intended to give an accurate measure of the relation between the EGRS and spacecraft as it moved on its trajectory past Jupiter, This information, along with the accurate knowledge of the Jupiter-relative spacecraft trajectory given by conventional doppler data near the encounter, was intended to give an accurate measurement of the Jupiter-EGRS angle. This angular information and narrow-band AVLBI passes taken using Voyager 2 and OJ 287 were to predict the Voyager 2 Jupiter encounter more accurately than conventional doppler data. The Voyager 2 encounter prediction could be verified with the accurate knowledge obtained after encounter from conventional doppler. An accurate encounter prediction would by implication verify the accuracy of the AVLBI data used in the demonstration.

III. Data Acquisition

To perform the demonstration, narrow-band VLBI data passes were scheduled during several weeks before and after the Jupiter encounter of each Voyager spacecraft. The passes were scheduled on a noninterference basis with normal Voyager operation, Twenty-five passes were scheduled on Voyager 1 between 27 January (DOY 027) and 5 April (DOY 095) 1979. Thirty-three passes were scheduled on Voyager 2 between 3 April (DOY 093) and 6 August (DOY 218). Of these, 22 passes had data quality sufficient to permit further processing. Figure 2 shows the passes analyzed in relation to the two Jupiter encounters.

The data were taken with VLBI equipment at each DSS. The equipment consists of radio frequency hardware to reduce the incoming S- or X-band signal to a 0- to 2-MHz band. This band is sampled, digitized, and recorded on video tape at a rate of 4 Mbits/s. The signal mixing and sampling are all controlled by each station's frequency standard, usually a hydrogen maser. Both the frequency standard and the instrumentation path delay must be stable to $\Delta f/f \leqslant 2 \times 10^{-14}$ for the measurements to be successful. The tapes were shipped to JPL for processing.

IV. Data Processing

The data processing steps necessary for the reduction of narrow-band AVLBI are shown in Fig. 3. Each step in the process will be discussed.

A. Correlation

Each tape contains approximately one hour of 4 Mbits/s data. To proceed with the data reduction, this huge volume of bits(up to 10^{11} per pass) must be reduced to more manageable proportions. This initial reduction is done by processing the tapes on the CIT-JPL Mark II VLBI correlator at Caltech (Ref. 4).

Briefly, the correlator operates by computing the geometric delay and delay rate between the stations, offsetting the bit streams by the proper amount and then multiplying the streams together. The resulting fast fringes are slowed by a phase model that includes the expected delay rate and the local oscillator frequencies. The output of the correlator is one-second (typically) averages of the sine and cosine of the differenced (residual) phase between the cross-correlated signals and the model. The correlator operates at the 4 Mbits/s rate at which the data were recorded so that correlation, once the clock and frequency offsets are determined, requires the same length of time as the observations.

The correlator was developed to work with broad-band white noise signals that fill the 2-MHz channel. However, the spacecraft carrier is a very narrow, and when considered over the 2-MHz channel, a very weak signal. To overcome the latter problem, advantage was taken of the narrowness of the signal by using local-model correlation, The correlator was adapted so that the phase model could be represented by a polynomial. The spacecraft data were then correlated against an effectively noise-free polynomial model of the phase at each station. These phases were differenced later in the data processing to produce interferometric phase like that obtained in the EGRS cross correlation. The use of local-model correlation produced a very narrow effective bandwidth, and thus, a high signal-to-noise ratio (SNR).

The polynomial model used for local-model correlation had to be reasonably accurate. The predicted received frequency had to be accurate to a few hertz and the frequency rate accurate to -0.1 Hz over a several hour pass. The polynomials were generated using the best spacecraft trajectory available and a current earth platform and troposphere model.

B. Phase Tracking

The correlator output is a magnetic tape that contains the sine and cosine of the residual phase at l-s (typically) intervals, along with time tags, model phase and delay, and housekeeping information, The data are treated scan by scan. A scan is broken up into 5 to 100 sections for fitting. The sine and cosine values for each section are fit by least squares to a function of the form A exp $i(\omega t$ t $\phi)$, where the initial values for the fit are obtained from a fast Fourier transform and/or the previous section. The value of the argument of the exponential ***evaluated at the*** *midtime* is the residual phase for the section, and ω is the residual fringe frequency. Further description of the phase tracking process can be found in Ref. 5.

The two spacecraft data streams (one for each station) can be differenced either before or after phase tracking. After phase tracking, the residual phase for each section is added to the model phase to obtain the total phase.

C. Observable and Partial Calculation

The separate spacecraft and EGRS data streams now form the observable for a standard orbit determination process. Using the best available estimate of the spacecraft ephemeris and the EGRS position, the observables (phase) and partial derivatives of the observables with respect to the parameters to be used in estimation are calculated. The program REGRES, from JPL's Orbit Determination Program set (Ref. 6) was used for this step. The observable phase calculated by REGRES is now subtracted from the total observed phase to obtain a new residual phase, hereinafter called REGRES residuals.

D. Media Calibration

Transmission media (troposphere, ionosphere, and solar wind) are significant error sources in radio tracking. A key feature of AVLBI is that the data are expected to be largely self-calibrating due to the differencing of data streams. However, to remove large, easily modelled phase rates that might interfere with phase tracking or phase connection, calibrations are applied to the data. A slab model of the troposphere was used in the correlation for both spacecraft and EGRS. Polynomials representing the line-of-sight phase change through the ionosphere to each source, based on Faraday rotation measurements from geostationary satellites, are subtracted from the REGRES residuals.

E. Phase Connection

Recall that each data stream for the spacecraft and EGRS are segmented into disconnected scans of seven minutes. The information content of narrow-band VLBI is strongly dependent on a continuing time history of phase (Refs. 1 and 2). Hence, each data stream must be connected.

The residual phase output from the phase tracking software has an ambiguity. with respect to that in the previous scan of 1 cycle. Hence the REGRES residuals have the same ambiguity. Phase connection consists of deciding upon the number of integer cycles that should be added or subtracted from each scan (after the first) such that the resulting residual phase has a smooth behavior (see Fig. 4). Numerical algorithms designed to determine the residual phase rate in ***the*** gap between two consecutive scans are used to aid in phase connection, One such algorithm is described in Ref. 7.

In addition, "connected" phase plots are examined to heuristically correct seemingly incorrect phase connections. Nevertheless, phase connection between two consecutive scans can still be in doubt as indicated in Fig. 4. When this occurs, the question arises as to whether it is better to leave it disconnected or to run the risk of having a misconnected pass. To answer this question a comparison was made between the effects of disconnecting a pass and of misconnecting it.

Figure 5 shows the results of a covariance analysis comparing misconnection and disconnection for a pass taken on the Goldstone/Madrid baseline at the declination and scan length of the demonstration. Both a long pass (4.75 hours, Fig. 5b) and a short pass (2.65 hours, Fig. 5a) are shown. The larger curves show the error in the determination of the spacecraft-EGRS angular separation for a single misconnection of one cycle vs the location in the pass of the misconnection. On the long pass, the error can be as great as the expected data accuracy (0.05 μrad). On the short pass, a single misconnection is disastrous! The error can be as large at 0.2 μrad with an expected error of 0.14 μrad in right ascension and 0.07 μrad in declination.

For a single disconnection during the pass, the one-sigma error resulting from a conservative 3-cm (1 σ) Gaussian phase noise is shown. The statistical error is an order of magnitude lower than the misconnection error. Consequently, it is far better to discard a doubtful connection between two scans than make a mistake and misconnect.

Figure 6 shows the angular separation errors due to a conservative 3-cm phase noise as functions of the number of disconnected segments in the pass for the same long and short passes, It is observed that, with 3-cm phase noise, the error in each component will not exceed 0.02 μrad until the pass is disconnected into seven segments for the long pass. This implies that even with every third scan left disconnected, the effects of phase-type noise remain acceptable. For a totally disconnected long pass, the error becomes 0.17 μrad in each

component, clearly unacceptable. The short pass appears to be acceptable for 1, 2, or 3 segments. Without phase connection over such a pass, the expected angular separation errors are 0.38 μrad in right ascension and 0.21 yrad in declination.

F. Differencing

Finally, the data streams, in the form of REGRES residuals and partials, are differenced. Since the differencing is intended to cancel common errors, the data streams are offset in time to maximize the cancellation. Two major error sources are the troposphere and ionosphere. The maximum cancellation of these errors for sources separated in right ascension and declination occurs for a time offset in minutes of

$$\Delta t = 4\Delta\alpha + 2.8\Delta\delta$$

where An! and A6 are the differences in degrees in right ascension and declination. A time offset of $\Delta t = 4\Delta\alpha$ also minimizes the sensitivity of AVLBI to station location errors. A linear phase drift in the instrumentation will be removed by differencing regardless of the time offset. However, nonlinear phase variations such as a clock frequency drift will be enhanced by the time offsetting. (See the error analysis discussion in Ref. 1).

The optimum time offset could not be realized with the demonstration data. To difference a scan of spacecraft data with a scan of EGRS data, an offset must be an odd integer times 7 minutes. The time offsets available are shown in Fig. 2. The available offset nearest the computed offset was considered optimal for that pass.

The differenced phase history is examined visually for discontinuities, usually at several time offsets including the optimal one. If a discontinuity shows up clearly, the individual phases are reexamined and corrected. It should be noted that there is a disconnection in the differenced phase whenever there is a disconnection in phase from either source. Thus, if there is one disconnection in the phase of each source, there will be two in the difference, i.e., three segments — the maximum number for usable data from short passes.

G. Parameter Estimation

The last step in the data processing is that of parameter estimation. The VLBI residuals and partials (possibly along with other data) are now input to an orbit determination filter where selected parameters are estimated.

To assess the consistency of the 22 passes, the EGRS right ascension α and declination δ were estimated for each pass. The spacecraft parameters were held fixed, so that with an accurate spacecraft trajectory, the solutions should cluster within the accuracy of the data. The passes were differenced with varying time offsets. Passes were phase connected with various algorithms; they were disconnected at points where connection seemed in doubt. The scatter of the α, δ solutions remained essentially the same for different data treatments.

Figure 7 shows the scatter of seven Voyager 1 passes and ten Voyager 2 passes resulting from a set of a, δ solutions. Right ascension and declination are shown separately vs time. The shaded region represents a conservative estimate of the uncertainty of the spacecraft trajectory. The "true" spacecraft trajectory would be represented by a straight line within the shaded region. Clearly, the scatter in the solutions are an order of magnitude larger than the expected 0.05 radians. The magnitude of the scatter and lack of a trend indicate that the spacecraft trajectory error is not contributing to the large scatter.

V. Discussion

The results of the Voyager AVLBI demonstration have not fulfilled the promise of the original error analysis. There are several reasons why the observed error is nearly a factor of 10 larger than originally predicted. Basically, the reasons are that the passes were shorter and the individual error sources were larger than was anticipated. Figure 6 clearly illustrates the effect of shorter passes by comparing covariance analyses for passes of 21 scans (4.75 hours) and 12 scans (2.65 hours). The predicted error is about a factor of 3 larger for the shorter pass. The shorter pass is typical of the actual observations, while the original error analysis was done for the longer pass.

Two major error sources for AVLBI are the transmission media, particularly the ionosphere, and the station instrumentation, Four passes of Voyager 2 data have dual-frequency (S- and X-band) data, which provide a direct measurement of the charged-particle-induced phase change. These measurements were compared to the Faraday polynomial calibrations. Assuming that there are no large instrumental effects in the SX data, the comparisons show 5- to 7-cycle differences over a pass between the actual line of sight phase change and the Faraday polynomial for each source. When the data are differenced between sources, most of this accumulation is removed, but discrepancies of about 1 cycle remain independent of time offsets. Thus, the differenced data calibrated with the Faraday polynomials are likely to contain false signatures of at least l-cycle accumulation from transmission media. This exceeds the total original error allocation by a factor of 2.

It is thought that the effect of false signatures in the Faraday calibrated differenced data may be even larger in the

Voyager 1 data where one station went through the day-night ionosphere transition during the observations. Because the Faraday polynomials are of relatively low order, they do not capture the rapid recombination of the ionosphere at the day-night transition. During a day-night transition, it is likely that the difference between the polynomial and the line of sight values will be larger than at other times, and the error cancellation between the 1 0-deg separated sources will be less. One might therefore expect errors of 2 to 3 cycles in the differenced data over a pass.

A second possible source of error in the observations is phase variations in the receiver chain and/or fluctuations in the 'stations' frequency standards. No direct measurements of the frequency standards are available. Equipment to measure the instrumental phase was available only at the Goldstone station and only for the latter part of the demonstration. Some of these data have been examined, and no large effects are apparent. It is interesting to consider what sort of instrumental errors would affect the data. Because of the data differencing, linear phase drifts have no effect, but linear frequency drifts do. A frequency drift of only 5 parts in 10^{14} could contribute 1 cycle to the accumulated phase in the differenced data. Similarly, a phase wander with an amplitude of 1 cycle and a period of a few hours could cause a l-cycle error in the differenced data. Both of these effects come about because of the time offsetting, which is done in the data processing to minimize transmission media errors.

Note that both the media and instrumental errors discussed here are accumulated over a pass and thus go directly into the solutions unlike the phase noise used in the covariance analyses shown in Figures 5 and 6. An order of magnitude estimate of the effect of accumulated errors can be obtained from the curve for misconnections in Fig. 5a; it shows that a l-cycle error gives a solution error of about 0.1 μrad. This is consistent with the above discussion of media errors of 1 to 3 cycles and consistent with the observed scatter of the solutions,

As was pointed out previously, phase connection is both difficult and extremely important. Transmission media and instrumental errors can not only contribute to solution errors in their own right, but can also cause mistakes in phase connection. In this case, rapid local variations in the phase rate are of the most concern. The SX data show that the ionosphere may have small scale irregularities on the order of 1/4 cycle (S-band) in a few minutes. Since the effect is only 3/1 1 as large at X-band, X-band data are likely to be correctly connected. Thus, S-band data calibrated with SX are likely to be much more reliable than when they are calibrated with Faraday polynomials.

The foregoing discussion makes it clear that the data actually acquired were not in line with the demonstration's original goals. The most significant problem with the actual data is the shortness of the passes. The data errors encountered probably would have allowed solutions at the 0.1-μrad level with passes $>$ 4.5 h in length. On the other hand, it is very likely that the data errors would have been smaller if the source separation had been smaller. Tests will soon begin to investigate data · errors as a function of source separation. Therefore, while the demonstration did not meet its goals, it did provide a much clearer understanding of the problems of navigating with AVLBI and what sort of system and data acquisition procedures are needed to reach angular accuracies of 0.05 μrad.

References

1. Brunn, D. L., et al., "AVLBI Spacecraft Tracking System Demonstration: Part 1. Design and Planning," ***DSN Progress Report, 42-45, March*** and ***April 1978***, pp. 11 l-132, Jet Propulsion Laboratory, Pasadena, Calif.

2. Curkendall, D. W., "Radio Metric Technology for Deep Space Navigation: A Development Overview," paper 78-1395 presented at the AIAA/AAS Astrodynamics Conference, Palo Alto, Calif., August 7-9, 1978.

3. Melbourne, W. G., and Curkendall, D. W., "Radio Metric Direction Finding: A New Approach to Deep Space Navigation," paper presented at the AAS/AIAA Astrodynamics Specialist Conference, Jackson Hole, Wyoming, September 7-9, 1977.

4. Thomas, J. B., "Cross Correlation and Fringe Stepping for a Multistation Correlator," Engineering Memo 3 15-23, March 15, 1977. Jet Propulsion Laboratory, Pasadena, Calif. (JPL internal document.)

5. Thomas, J. B., ***An Analysis of Long Baseline Radio Interferometry, Part III,*** Technical Report 32-1526, Vol. XVI, pp. 47-64. Jet Propulsion Laboratory, Pasadena, Calif.

6. Ekelund, J. E., "The JPL Orbit Determination Software System," paper 79-l 11 presented at the AAS/AIAA Astrodynamics Specialist Conference, Provincetown, Mass., June 25-27, 1979.

7. wu, s. c., "Connection and Validation of Narrow-Band AVLBI Phase Observation," ***DSN Progress Report*** 42-52, pp. 13-20. Jet Propulsion Laboratory, Pasadena, Calif., August 15, 1979.

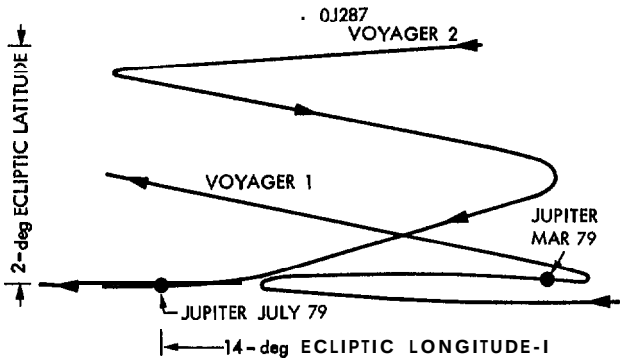

Fig. 1. The Voyager Spacecraft trajectories as seen from Earth

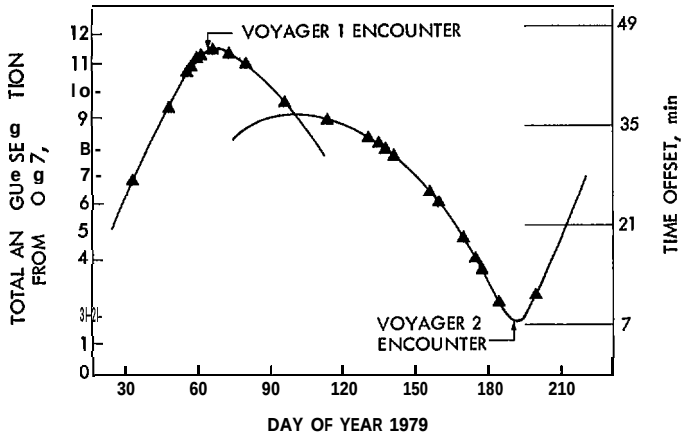

Fig. 2. The Voyager ΔVLBI passes and the Voyager-OJ 237 angular separation

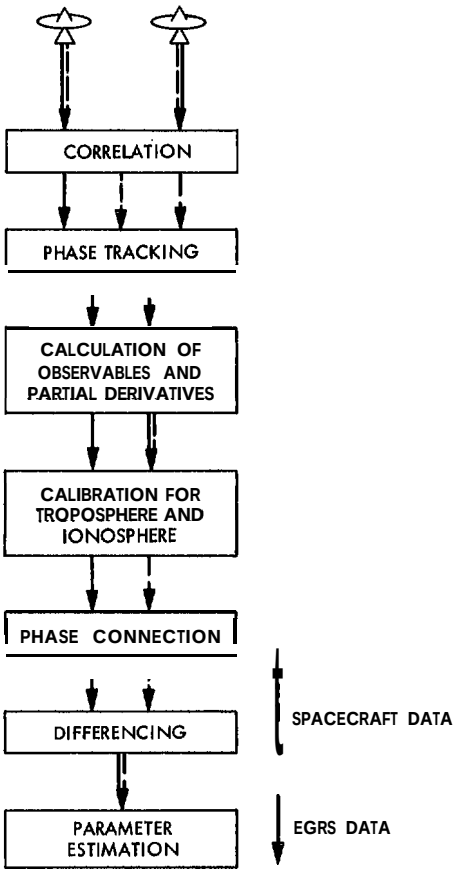

Fig. 3. Narrow-band AVLBI data processing steps

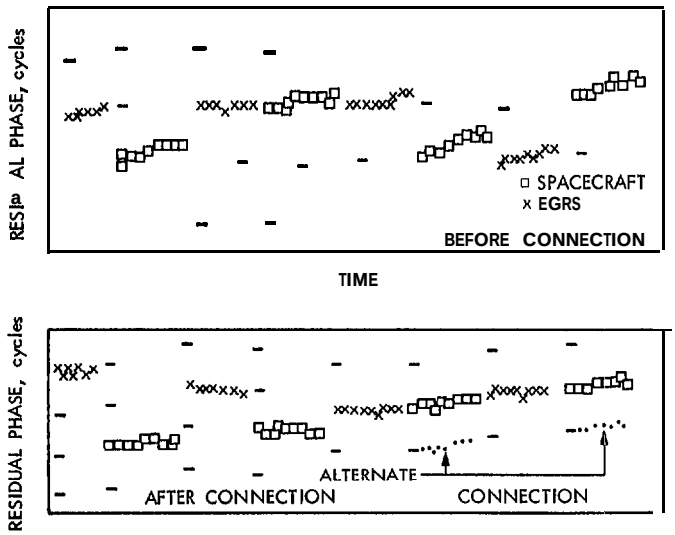

Fig. 4. Alternating scans of Voyager 2 and OJ 287 residual phase. The marks are spaced at l-cycle increments from the first-phase residual of each scan. Note the alternative phase connection shown

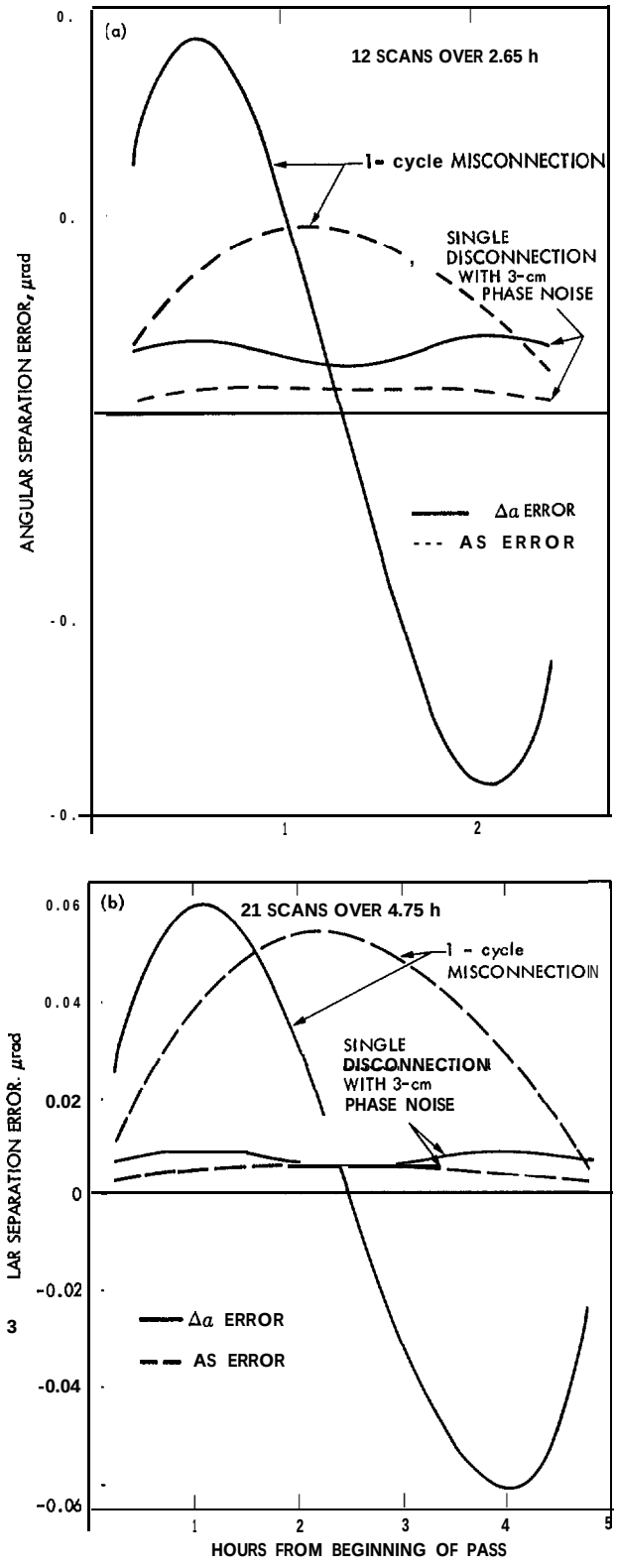

Fig. 5. Comparison of errors due to phase misconnection and disconnection (a) for a short pass (2.65 h), (b) for a long pass (4.75 h). Note the scale difference between (a) and (b)

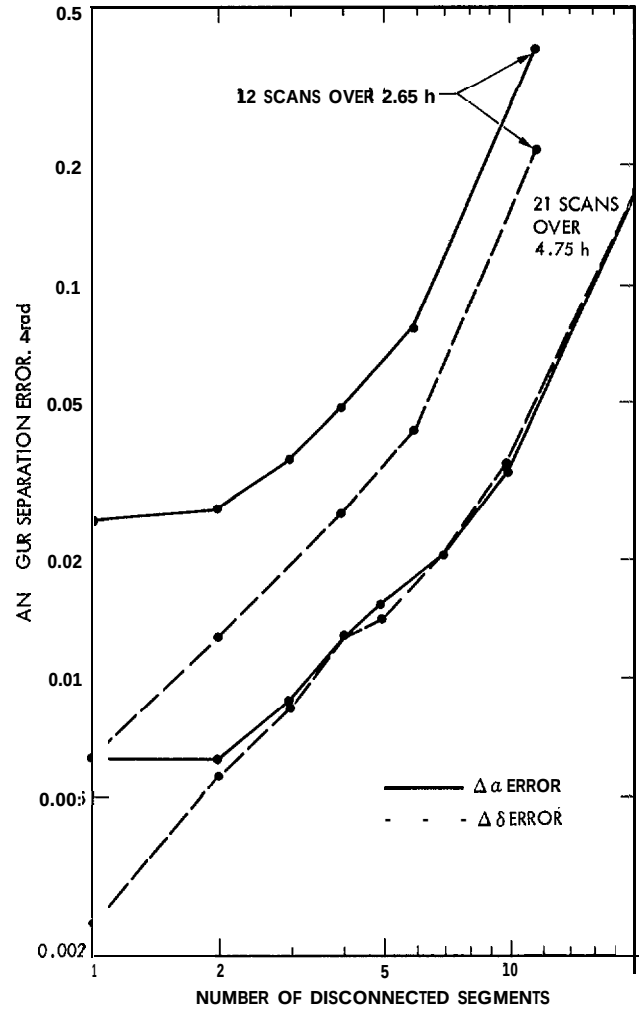

Fig. 6. Effects of phase noise on a multiply disconnected pass

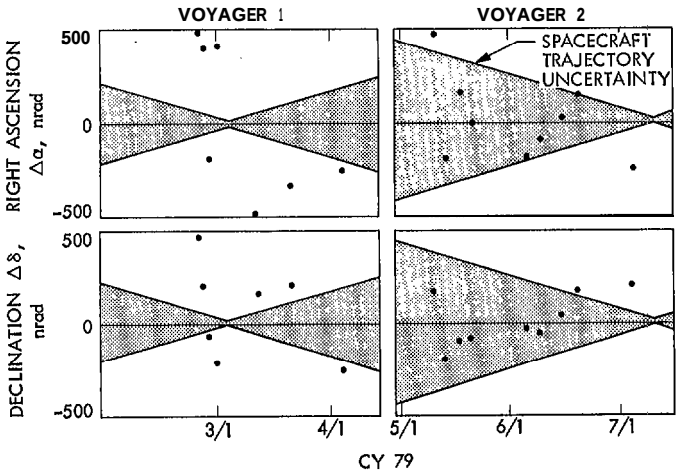

Fig. 7. Scatter plot of right ascension and declination of narrow-band ΔVLBI